8.2 STABILITY OF SMALL SELF-INTERSTITIAL CLUSTERS IN TUNGSTEN — W. Setyawan, G. Nandipati, and R. J. Kurtz (Pacific Northwest National Laboratory)

OBJECTIVE

The objective of this research is to explore the structures of small clusters of interstitials in W. These structures will serve as representative configurations that will be used to calculate the binding of such clusters to transmutation products in W. The results will be used to inform kinetic Monte Carlo simulations of radiation damage accumulation containing transmutation products, in particular Re and Os.

SUMMARY

Density functional theory was employed to explore the stability of interstitial clusters in W up to size seven. For each cluster size, the most stable configuration consists of parallel dumbbells. For clusters larger than size three, parallel dumbbells prefer to form in a multilayer fashion, instead of a planar structure. For size-7 clusters, the most stable configuration is a complete octahedron. The binding energy of a [111] dumbbell to the most stable cluster increases with cluster size, namely 2.49, 3.68, 4.76, 4.82, 5.47, and 6.85 eV for clusters of size 1, 2, 3, 4, 5, and 6, respectively. For a size-2 cluster, collinear dumbbells are still repulsive at the maximum allowable distance of 13.8 Å (the fifth neighbor along [111]). On the other hand, parallel dumbbells are strongly bound together. Two parallel dumbbells in which the axis-to-axis distance is within a cylindrical radius of 5.2 Å still exhibit a considerable binding of 0.28 eV. The most stable cluster in each size will be used to explore interactions with transmutation products.

PROGRESS AND STATUS

Method

VASP [1, 2] software was used to perform the quantum calculations within the density functional theory (DFT) framework. Core electrons are modeled with accurate projector-augmented-wave pseudopotentials [2]. Electrons in 6s and 5d states are treated as valence electrons. Perdew-Burke-Ernzerhof formulations [3] were employed for the exchange-correlation functionals. Defect formation energies were calculated using cubic 5x5x5 supercells of tungsten's bcc unit cell. A Monkhorst-Pack [4] k-points grid of 3x3x3 is sufficient to obtain accurate formation energies. The coordinates of atoms and box volume are optimized while maintaining cubic symmetry. In relaxed configurations, the forces are < 0.025 eV/Å and the external pressure < 0.5 kbar. At the end of the relaxations, a static calculation was performed to eliminate errors due to basis incompleteness associated with changes in the simulation cell. A convergence study of the defect formation energies of <111>, <110>, and <100> dumbbells was performed with respect to the energy cutoff (ENCUT) for the plane waves up to 350 eV. An energy cutoff of 250 eV was found to be sufficient to converge the formation energies of those dumbbells within 20 meV. Therefore, all subsequent calculations were performed with ENCUT = 250 eV.

Results

Size-2 Clusters

Figure 1a shows a pool of 10 lattice sites used to find unique configurations of size-2 clusters. This pool encompasses up to the fifth nearest-neighbor (nn) distance. A new option (synopsis *–pick*) was developed and added to our in-house utility code *axisvasp* to pick n = 2 site combinations out of the m = 10 sites. Subsequently, non-equivalent combinations are identified based on bond lengths. There are 5 unique 2-site combinations. A new option (synopsis *–dbdb*) was developed to build dumbbells at those sites. Note that the most stable dumbbell in W is a [111] dumbbell. Therefore, we explore clusters of <111> dumbbells. For size-2 clusters, a complete permutation of Miller indices (h = ±1, k = ±1, l = ±1) of the dumbbell's orientation is explored. There are 64 possible configurations out of which 23 are unique and subsequently relaxed. Figure 1b-1f shows the relaxed configuration of the five most stable clusters. The binding energy (E_b) needed to separate the two dumbbells is 2.49, 2.46, 1.99, 1.65, and 1.06 eV,

respectively. The most stable configuration is two [111] dumbbells separated at the third nn distance, with axis-to-axis distance of $a\sqrt{2}/\sqrt{3}$ = 2.60 Å (where a is the lattice constant). We refer the most stable cluster-2 configuration as MSC-2.

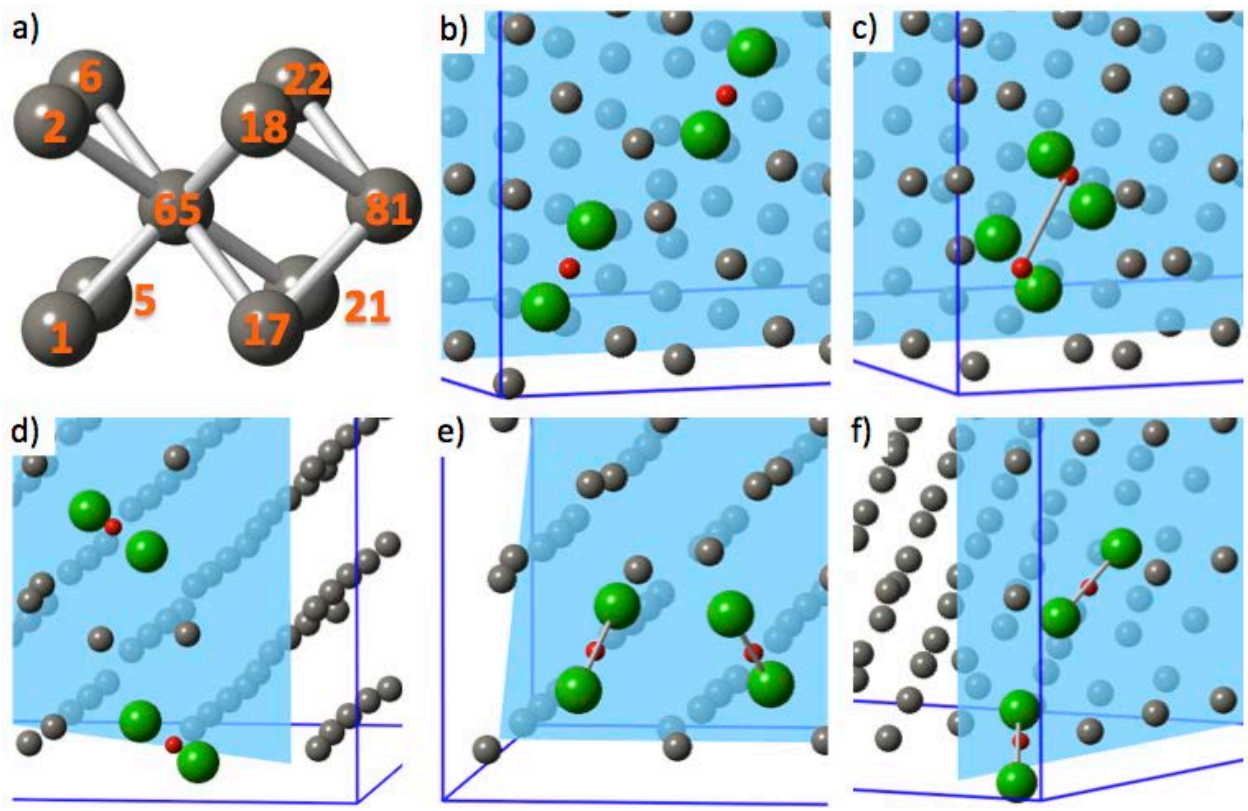

Figure 1. a) Lattice sites from which configurations of <111> dumbbells are searched. The five most stable structures of size-2 clusters are shown in b) to f) with binding energy of 2.49, 2.46, 1.99, 1.65, and 1.06 eV, respectively. The orientations are b) both [111], c) both [11-1], d) both [111], e) [111] and [11-1], and f) [111] and [1-11].

Two collinear [111] dumbbells are strongly repulsive. The farthest separation with a 5x5x5 supercell along the diagonal is $(5a\sqrt{3})/2$ = 13.8 Å (the fifth neighbor along [111]). At this distance, two collinear dumbbells still exhibit a binding energy of -1.26 eV. On the contrary, if the axes of the dumbbells are parallel, instead of collinear, the dumbbells are strongly binding (Figure 1b-1d). Note that in Figure 1b-1d, the axis-to-axis distance is always $a\sqrt{2}/\sqrt{3}$ = 2.60 Å. With the two [111] dumbbells separated at $2a/\sqrt{2}$ = 4.51 Å (the third nn) and axis-to-axis distance of $2a/\sqrt{2}$ = 4.51 Å, the binding is still strong, 0.78 eV. At a larger axis-to-axis separation of $2a\sqrt{2}/\sqrt{3}$ = 5.20 Å, [111] dumbbells separated at $a\sqrt{3}$ = 5.52 Å (the second neighbor along [111]) have a binding energy of 0.28 eV. This indicates that two parallel dumbbells within a cylindrical radius of 5.2 Å still exhibit a considerable binding of 0.28 eV.

Non-parallel <111> dumbbells such as the [111] and [11-1] pair can have significant binding as well, as shown in Figure 1e (E_b = 1.65 eV) and Figure 1f (E_b = 1.06 eV). However, the strongest binding is clearly between parallel <111> dumbbells. Therefore, for larger clusters, we focus on clusters of <111> parallel dumbbells.

Size-3 Clusters

Figure 2a shows the nine lattice sites from which the size-3 clusters are identified. Taking combinations of 3 out of 9 sites results in 84 combinations which reduces to 6 unique ones, namely (1, 65, 17), (1, 65, 18), (1, 65, 22), (1, 17, 18), 1, 17, 22), and (1, 18, 6). Permuting <111> orientations of the dumbbells at those unique sites results in 3,072 configurations, which reduces to 101 unique ones. Considering only the parallel orientations reduces the number to 13 configurations, which are then relaxed. Figure 2b-2f shows the relaxed configuration of the five most stable clusters. The binding energy with respect to a [111] dumbbell and MSC-2 is 3.68, 3.13, 2.56, 1.30, and 0.03 eV, respectively. The most stable cluster-3 (MSC-3) configuration consists of [11-1] dumbbells arranged on the (01-1) plane. From this result, we focus on the exploration of larger clusters created from initial configurations of [11-1] dumbbells on the (01-1) plane.

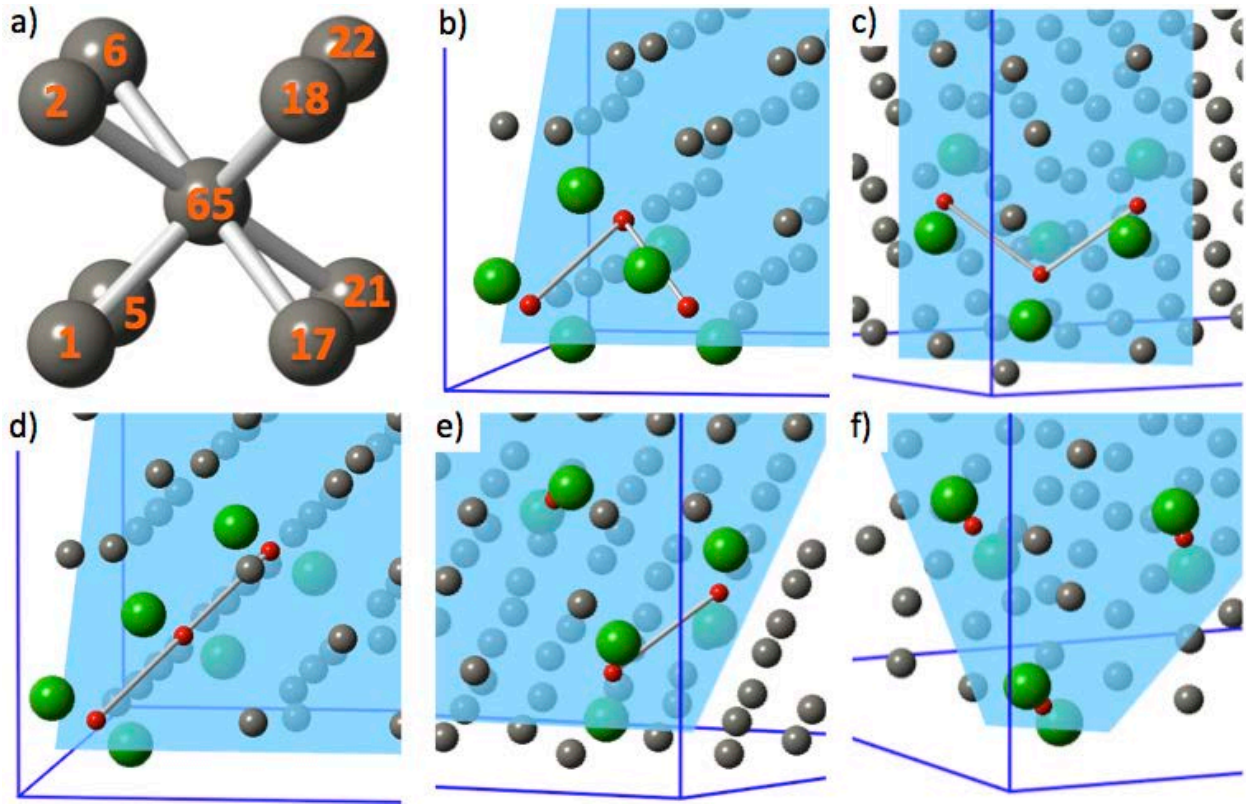

Figure 2. a) Lattice sites from which configurations of size-3 <111> parallel dumbbells are searched. The five most stable structures of size-3 clusters are shown in b) to f) with binding energy, with respect to a [111] dumbbell and the most stable size-2 cluster, of 3.68, 3.13, 2.56, 1.30, and 0.03 eV, respectively.

Size-4 Clusters

Figure 3a shows the 12 lattice sites from which the size-4 clusters are identified. Taking combinations of 4 out of 12 sites results in 495 combinations, which reduces to 90 unique ones. Then, [11-1] parallel dumbbells are placed at those 90 unique combinations of sites and the structures are relaxed. Figure 3b-3f shows the relaxed configuration of the five most stable clusters. The binding energy with respect to a [111] dumbbell and MSC-3 is 4.76, 4.67, 3.40, 2.76, and 2.74 eV, respectively. Figure 3b shows the most stable cluster-4 (MSC-4) configuration. Interestingly, even though all initial configurations are constructed with [11-1] dumbbells on (01-1) plane, i.e. planar configurations, the final structure of MSC-4 shows [11-1]

dumbbells arranged on 2 layers of the (10-1) plane. Arrows in Figure 3b indicate the projected location of three of the dumbbells onto one of the (10-1) layers.

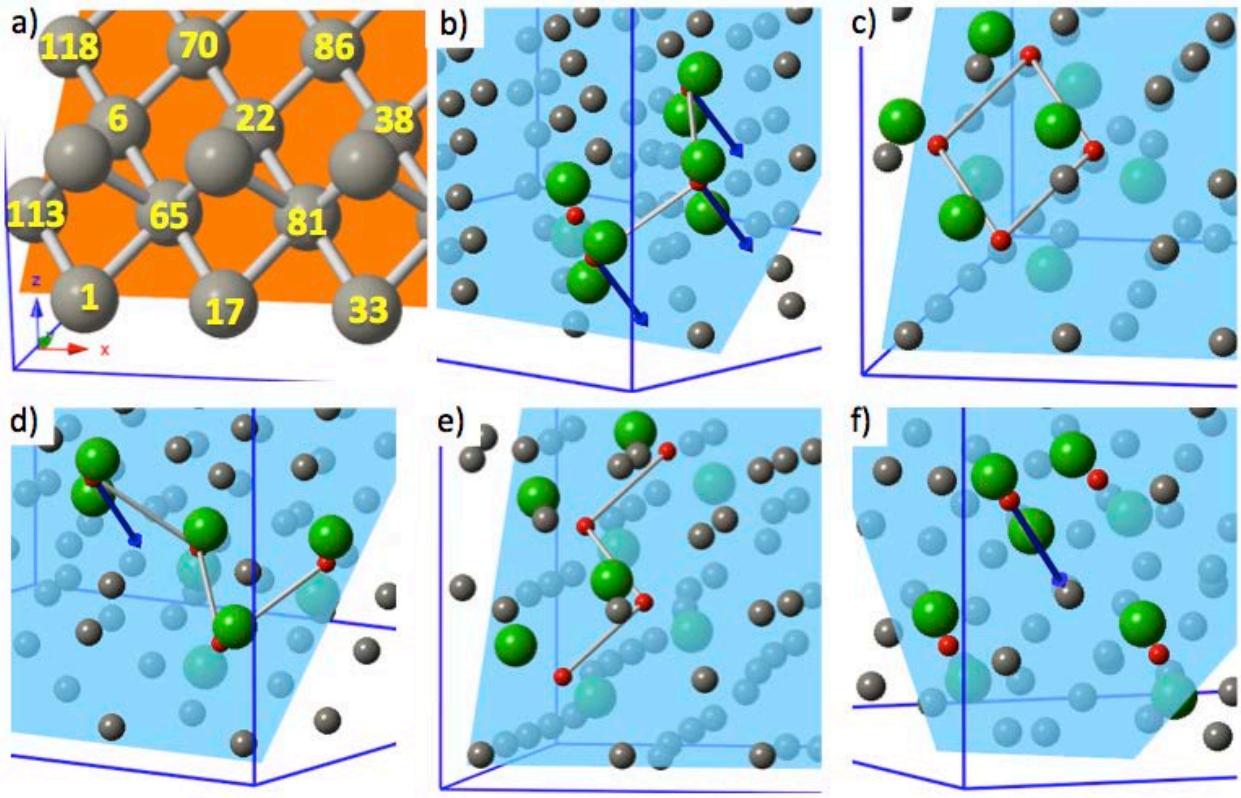

Figure 3. a) Lattice sites from which configurations of size-4 <111> parallel dumbbells are searched. The five most stable structures of size-4 clusters are shown in b) to f) with binding energy, with respect to a [111] dumbbell and the most stable size-3 cluster, of 4.76, 4.67, 3.40, 2.76, and 2.74 eV, respectively. Arrows indicate the projected location of dumbbells on to the shaded plane.

Size-5 Clusters

Size-5 clusters were found from the same 12 lattice sites as size-4 clusters. Taking combinations of 5 out of 12 sites results in 792 combinations, which reduces to 181 unique ones. Then, [11-1] parallel dumbbells are placed at those 181 unique combinations of sites and the structures are relaxed. Figure 4b-4f shows the relaxed configuration of five most stable clusters. The binding energy with respect to a [111] dumbbell and MSC-4 is 4.82, 3.89, 3.87, 3.47, and 3.42 eV, respectively. Figure 4b shows the most stable cluster-5 (MSC-5) configuration. Similar to MSC-4, the final structure of MSC-5 shows [11-1] dumbbells arranged on 2 layers of the (01-1) plane.

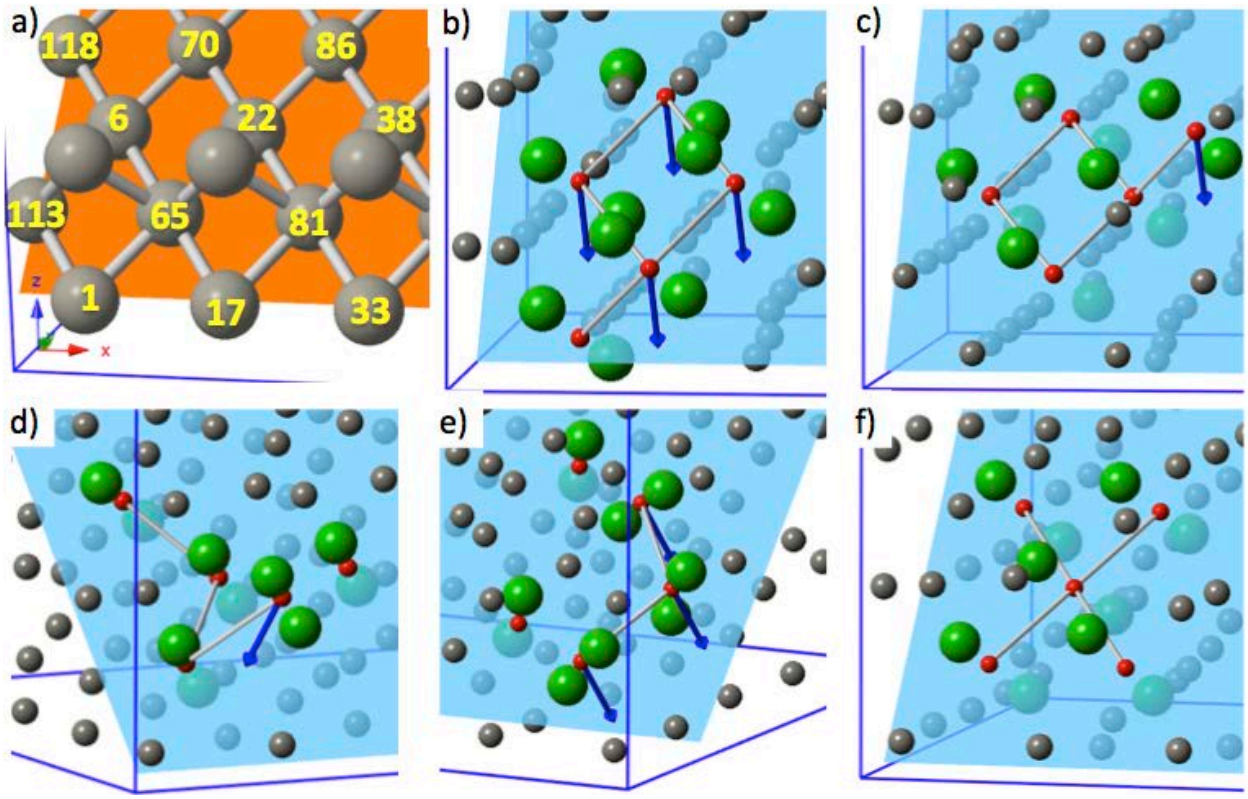

Figure 4. a) Lattice sites from which configurations of size-5 <111> parallel dumbbells are searched. The five most stable structures of size-5 clusters are shown in b) to f) with binding energy, with respect to a [111] dumbbell and the most stable size-4 cluster, of 4.82, 3.89, 3.87, 3.47, and 3.42 eV, respectively. Arrows indicate the projected location of dumbbells on to the shaded plane.

Size-6 Clusters

Size-6 clusters are found from the same 12 lattice sites as size-4 clusters. Taking combinations of 6 out of 12 sites results in 924 combinations, which reduces to 259 unique ones. Then, [11-1] parallel dumbbells are placed at these 259 unique combinations of sites and the structures are relaxed. Figure 5b-5f shows the relaxed configuration of five most stable clusters. The binding energy with respect to a [111] dumbbell and MSC-5 is 5.47, 5.13, 4.97, 4.97, and 4.92 eV, respectively. Figure 5b shows the most stable cluster-6 (MSC-6) configuration. The final structure of MSC-6 shows [11-1] dumbbells arranged on 2 layers of the (110) plane.

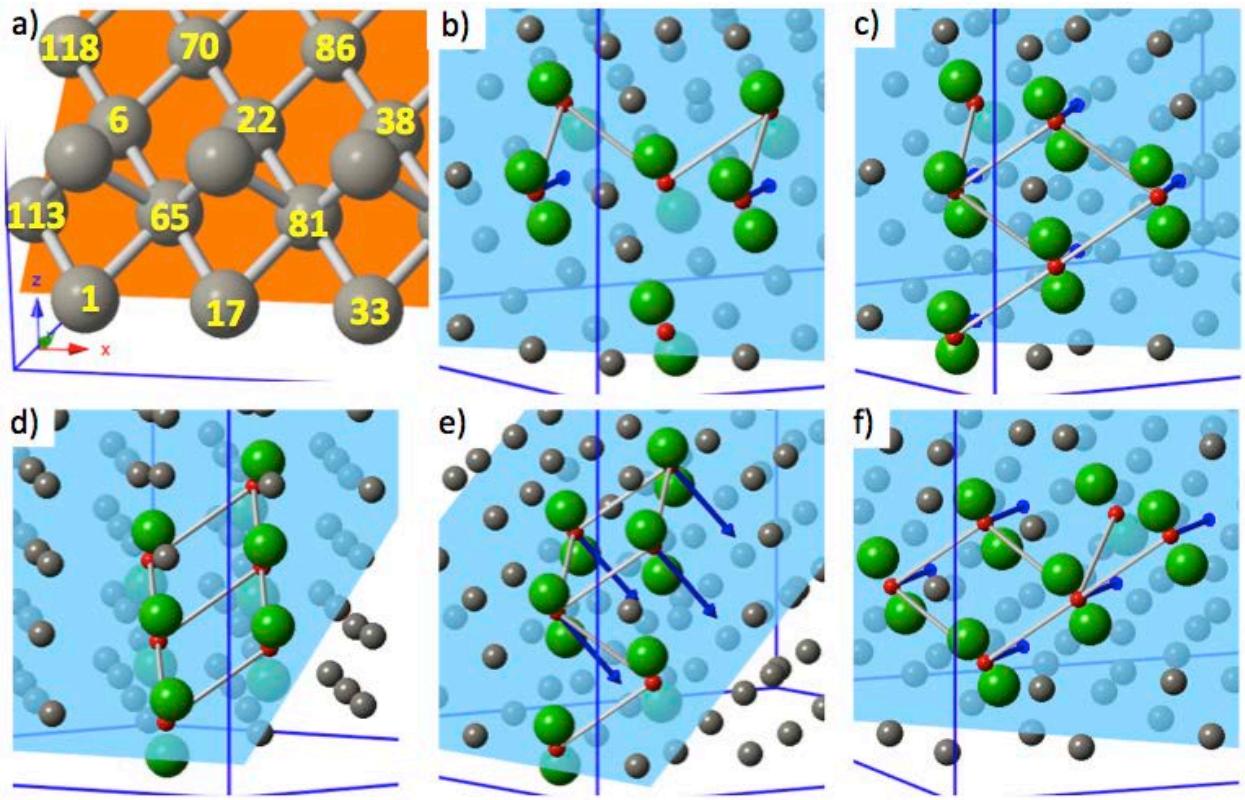

Figure 5. a) Lattice sites from which configurations of size-6 <111> parallel dumbbells are searched. The five most stable structures of size-6 clusters are shown in b) to f) with binding energy, with respect to a [111] dumbbell and the most stable size-5 cluster, of 5.47, 5.13, 4.97, 4.97, and 4.92 eV, respectively. Arrows indicate the projected location of dumbbells on to the shaded plane.

Size-7 Clusters

Size-7 clusters are identified from the same 12 lattice sites as size-4 clusters. Taking combinations of 7 out of 12 sites results in 792 combinations, which reduces to 269 unique ones. Then, [11-1] parallel dumbbells are placed at these 269 unique combinations of sites and the structures are relaxed. Figure 6b-6f shows the relaxed configuration of five most stable clusters. The binding energy with respect to a [111] dumbbell and MSC-6 is 6.85, 5.30, 5.27, 4.29, and 4.18 eV, respectively. Figure 6b shows the most stable cluster-7 (MSC-7) configuration. The final structure of MSC-7 shows [11-1] dumbbells forming a complete octahedron.

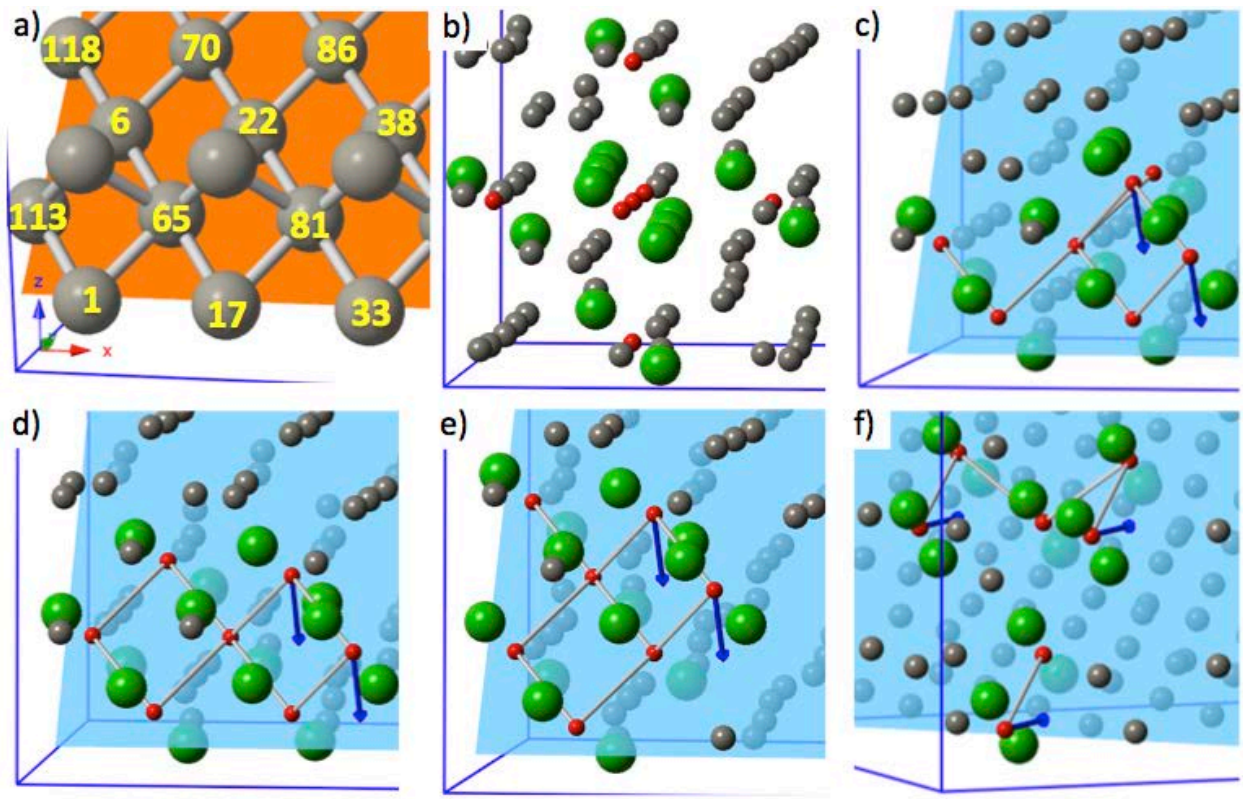

Figure 6. a) Lattice sites from which configurations of size-7 <111> parallel dumbbells are searched. The five most stable structures of size-7 clusters are shown in b) to f) with binding energy, with respect to a [111] dumbbell and the most stable size-6 cluster, of 6.85, 5.30, 5.27, 4.29, and 4.18, respectively. Arrows indicate the projected location of dumbbells on to the shaded plane.

The stability of interstitial clusters up to size seven has been obtained. The results show that the binding of a [111] dumbbell to interstitial clusters increases with the size of the clusters. For each cluster size, the most stable configuration has been obtained and will be used to explore the interaction of such clusters with transmutation products such as Re and Os.

This research has been supported by the U.S. Department of Energy, Office of Science, Office of Fusion Energy Sciences (DE-AC06-76RL0-1830).

References

[1] P. E. Blöchl, Phys. Rev. B 50 (1994) 17953.
[2] G. Kresse and D. Joubert, Phys. Rev. B 59 (1999) 1758.
[3] J. P. Perdew, K. Burke and M. Ernzerhof, Phys. Rev. Lett. 77 (1996) 3865.
[4] H. J. Monkhorst and J. D. Pack, Phys. Rev. B 13 (1976) 5188.